Selenium-Facilitated Antioxidant System Response in Zea Mays Seedlings Under Reactive Oxygen Species-Induced Stress

Afshan Shahzadi, Alishba Sadia, Ubaidullah, Ayesha Siddiqa
Institute of Microbiology & Molecular Genetics, University of the Punjab, Lahore, Pakistan
*** Correspondence:** ayesha.mmg@pu.edu.pk

Citation | Shahzadi. A, Sadia. A, Ubaidullah, Siddiqa. A, "Selenium-Facilitated Antioxidant System Response in Zea Mays Seedlings under Reactive Oxygen Species Induced Stress", IJASD, Vol. 8 Issue. 1 pp 1-20, Jan 2026

Received| December 12, 2025 **Revised|** December 29, 2025 **Accepted|** Jan 07, 2026 **Published|** Jan 13, 2026.

Selenium (Se) is a vital micronutrient that plays an important role in metabolic, cellular, and physiological activities. Its deficiency can hinder growth, immunity, fertility, and cellular structure. This study inspected the effect of selenium and hydrogen peroxide-induced oxidative stress on the Zea mays L. seed germination, growth, and antioxidative activity. Soil samples were collected produced significant selenite-resistant and auxin-producing strains. These isolates were further tested for selenite reduction, plant growth-promoting characteristics, and other biochemical properties. Optimal selenite reduction was achieved at pH 7 at a temperature of 37°C, and up to 1900 μg ml^{-1} concentration. Responses to high selenite concentrations fluctuated from strain to strain, including variations in growth, auxin production, and antimicrobial activity against Bacillus thuringiensis. After six days of exposure to 20 mM H_2O_2, a considerable rise in root malondialdehyde content was seen, suggesting the presence of oxidative stress. Generally, selenium improved antioxidative defense mechanisms and tolerance to H_2O_2 stress. These findings deduce that PGPR inoculation significantly reduced H_2O_2 and MDA levels while enhancing POD activity and seedling growth under oxidative stress.

Keywords: Antioxidative Defense, Bacillus, Hydrogen Peroxide, Seedling Growth, Selenium, Oxidative Stress, Plant-Microbe Interactions, Zea Mays

Introduction:

Oxidative stress is a key problem in plant physiology, occurring when ROS levels surpass the capacity of detoxification processes of the plant cell. H_2O_2 acts as a key ROS that regulates growth, differentiation, and defense responses in plants in low to moderate levels. However, at high levels, it can cause oxidative damage to lipids, nucleic acids, and proteins by mediating processes such as lipid peroxidation [1][2]. In Zea mays (maize), environmental stresses like drought, salinity, and waterlogging often induce overproduction of H_2O_2, triggering the production of antioxidant enzymes like superoxide dismutase, catalase, and peroxidases to reestablish redox balance [3][4].

Selenium is a trace element that causes a "double-edged sword" effect in plants. While not severely essential for most plant species, selenium can protect against abiotic stress produced by ROS by increasing the antioxidant defense system, but at higher concentrations, selenium becomes toxic, and which results in the production of excessive oxidative stress [5]. High selenium levels in Zea mays seedlings have been reported to reduce growth, lower chlorophyll content, and increase malondialdehyde, a lipid peroxidation indicator, content while also altering the reactions involving enzymes such as superoxide dismutase, guaiacol peroxidase, and catalase [6]. Selenium can be supplemented either by priming or as a nanoparticle. Selenium and H_2O_2 have an interesting effect on ROS metabolism during

antioxidant pathways in nature, as they might enhance stress tolerance by enhancing the activity of antioxidant enzymes and reducing overall H_2O_2 levels [7][8].

Several modern studies have explored how selenium affects Zea mays' functioning during stressful conditions. In salt-stressed maize, foliar application of selenium enhanced growth, photosynthetic pigments production, antioxidant enzyme activities, and alterations in ionic homeostasis (e.g., raising K^+ content, regulating Na^+ compartmentalization via ZmNHX1). A different study found that seed priming (with Selenium nanoparticles) boosted Zea mays seedling resistance to salt stress, increasing antioxidant capacity while decreasing oxidative damage.

Exogenous administration, also called priming of H_2O_2, has been widely explored to improve stress tolerance in maize. Priming maize seeds with H_2O_2 promoted seed germination and growth under drought conditions. It also increased antioxidant enzyme activity (catalase, guaiacol peroxidase, and superoxide dismutase), reduced malondialdehyde content, and increased proline and soluble sugars levels, which are osmoprotectants [9]. Zea mays treated with H_2O_2 displayed greater photosynthetic performance, net carbon assimilation, more open stomata, and enhanced photosystem II efficiency during waterlogging stress, leading to higher grain production [10]. Research advocates that seed priming with H_2O_2 and other compounds (e.g., proline) can enhance antioxidant responses during drought conditions.

The latest study has begun to investigate how selenium and H_2O_2 interact and control oxidative stress. Zea mays seeds, which were primed with selenium nanoparticles, reduced malondialdehyde and H_2O_2 levels as compared to non-primed seeds. This suggests that it can reduce overall oxidative stress by suppressing H_2O_2 accumulation and enhancing antioxidant mechanisms.

While selenium and H_2O_2 priming individually enhance oxidative stress tolerance in maize, limited information is available on the synergistic role of selenium-resistant PGPR under ROS-induced stress. This study uniquely integrates selenium-resistant rhizobacteria, H_2O_2 stress, and antioxidant regulation in Zea mays seedlings.

Study Objectives:

To isolate and characterize selenium-resistant rhizobacteria

To evaluate their multi-metal resistance and selenite reduction potential

To assess their effect on Zea mays seedling growth under H_2O_2 stress

To analyze oxidative stress markers (H_2O_2, MDA, POD) in supplemented seedlings

Materials and Methods:

All experimental work was conducted under sterilized conditions. Glassware, solutions, dyes, and media were sterilized at 121°C for 15 min under 15 psi pressure [11]. All chemicals were prepared using distilled water and handled according to laboratory safety protocols. Nutrient agar and broth were prepared according to established recipes and methods by dissolving the required ingredients in 1L distilled water, adjusting pH to 7, and autoclaving before use [12][13].

Isolation of Selenium-Resistant Bacteria:

Soil samples were serially diluted (10^{-1} to 10^{-9}) while 10^{-2}, 10^{-5}, and 10^{-9} dilutions were spread on N-agar supplemented with about 400µg/mL Na_2SO_3. After incubation at 37°C for 24 hrs, distinct colonies were selected and purified through quadrant streaking and incubated for 24 hrs. at 37°C. [14]

Cellular Morphological Characteristics via Staining:

Cellular morphology of the isolated bacteria was assessed using classical staining techniques. Gram staining, endospore staining, and cellular shape examination were

conducted to categorize isolates and detect endospore-forming species using standard microbiological procedures. [15][16][17].

Biochemical Characterization of Bacteria:

Each isolate was examined by using several biochemical tests, including catalase, oxidase, starch hydrolysis, citrate utilization, methyl red and Voges-Proskauer reactions, nitrate reduction, phosphate solubilization, ammonia production, auxin biosynthesis, and malonate utilization. Physiological and biochemical tests were conducted to characterize the metabolic capabilities of the isolates. Catalase activity was performed with 3% H_2O_2, and oxidase activity was determined by 1% tetramethyl-p-phenylenediamine [18][19]. Bacterial isolates were incubated on starch agar, Simmon's citrate agar, and Pikovskaya agar for starch hydrolysis, citrate utilization, and phosphate solubilization test, respectively [20][21]. The MR/VP test was performed on glucose phosphate media following established protocols [22][23][24]. Nitrate reduction test and ammonia production were done on nitrate broth and 4% peptone water, respectively [25][26]. Auxin production was quantified using L-tryptophan-supplemented broth and broth without L-tryptophan [27], and malonate production was performed using recorded protocols [28].

Antimicrobial Assay:

Mueller-Hinton agar was used to measure antimicrobial activity against Bacillus thuringiensis using standard disc-diffusion methods [29]. Sterile discs impregnated with test bacterial solutions were then placed onto Bacillus thuringiensis inoculated plates to screen bacterial isolates for antibacterial activity against specific indicator pathogens and incubated for 24 hours. After incubation, zones of inhibition were observed and recorded in mm. These results were also compared with conventional antibiotic sensitivity standards to examine for possible biocontrol application [30].

Selenite Reduction Assay:

Selenite reduction assay was performed using a colorimetric method. The first bacterial inoculum was given in falcons containing N broth and incubated for 48 hrs at 37°C in a shaking incubator (150 rpm). The formation of red precipitate after incubation indicated elemental selenium (Se^0) formation. Cells were pelleted at 5000 rpm for 10 min and washed twice with NaCl. The pellet containing selenium was resuspended in sterile water, and the optical density at 500 nm was used as an indirect measure of elemental selenium formation, with higher OD indicating greater reduction potential. This assay showed the detoxifying and metabolic abilities of these isolates under selenium stress. Thermal (28, 37, 45 °C) and pH (5, 7, 9) tolerance profiles under selenite stress were also investigated to identify the physiological adaptation. [31]

Cross-Metal Resistance Assay:

Cross-metal resistance was inspected to determine co-tolerance patterns among isolated strains [31]. Heavy metals such as Cobalt (Co) Copper (Cu), Iron (Fe), Lead (Pb), Lithium (Li), Magnesium (Mg), Manganese (Mn), Mercury (Hg), Nickel (Ni), Potassium dichromate ($K_2Cr_2O_7$) and Zinc (Zn) and were individually added to N-Agar plates using 1% stock solutions, or 400µg/mL [32][33][34][35][36][37][38][39]. Bacterial inoculum was delivered in the form of streaks, and plates were incubated for 24 to 48 hrs at 37 °C. The scores for growth intensity were recorded as (+) weak growth, (++) moderate growth, (+++) high growth, and (–) no growth. Metal-resistance profiles were used to evaluate environmental resilience and possible applicability in bioremediation of multi-metal contaminated environments.

Screening of Microbial Strains for Plant Growth-Promoting Properties:

Plant growth-promotion properties of isolates were observed under controlled laboratory conditions. The objectives of the tests were to examine how selenium affects

seedling growth and compare growth under various treatments, such as selenium, H_2O_2, and their mixture. In accordance with known PGPR inoculation procedures, bacterial inocula were made by cultivating isolates in nutrient broth at 28°C for 24 hours, followed by centrifuging, washing, and resuspending to around 10^2 CFU/mL. [40]. For other experimental setups, cultures were also grown in N-broth at 37°C for 24 hrs in a shaking incubator at 150 rpm. Post-incubation, cultures were centrifuged aseptically at 5000 rpm for about 5 min, with changes to centrifugation time and speed made according to strain-specific growth rates. The resulting pellets were rinsed with sterile distilled water, suspended, and their optical densities were standardized to 1.0 at 600 nm using a spectrophotometer. Seeds were surface-sterilized using 0.1% mercuric chloride, rinsed thoroughly with sterile distilled water, and inoculated by soaking in the prepared bacterial suspensions for 25-30 min [41]. Control seeds were only soaked in sterile distilled water for the same time period. Inoculated seeds were then placed on sterile petri plates lined with a double layer of moist filter paper. For the seedling growth experiments, 10 bacterial strains from each of two consortia were used. Each petri plate was labeled according to the provided treatment and contained healthy inoculated seeds placed on sterile, moistened filter paper. Treatments were divided into three groups, i.e., one with only selenium, one with only H_2O_2, and one with both selenium and H_2O_2. The plates were incubated at 37°C for 7 days in a dark chamber under carefully monitored laboratory conditions. The test groups received their respective treatments daily. After seven days, seedling growth parameters were measured, including root length (cm), shoot length (cm), and the quantity of root hairs. To guarantee optimal growth conditions, seedlings were handled with extreme care, measured precisely, and given water frequently. All seedling measurements were performed in triplicate (n = 3) with independent biological replicates. The effects of chemical treatments and bacterial inoculation on seedling development were assessed using data analysis [42].

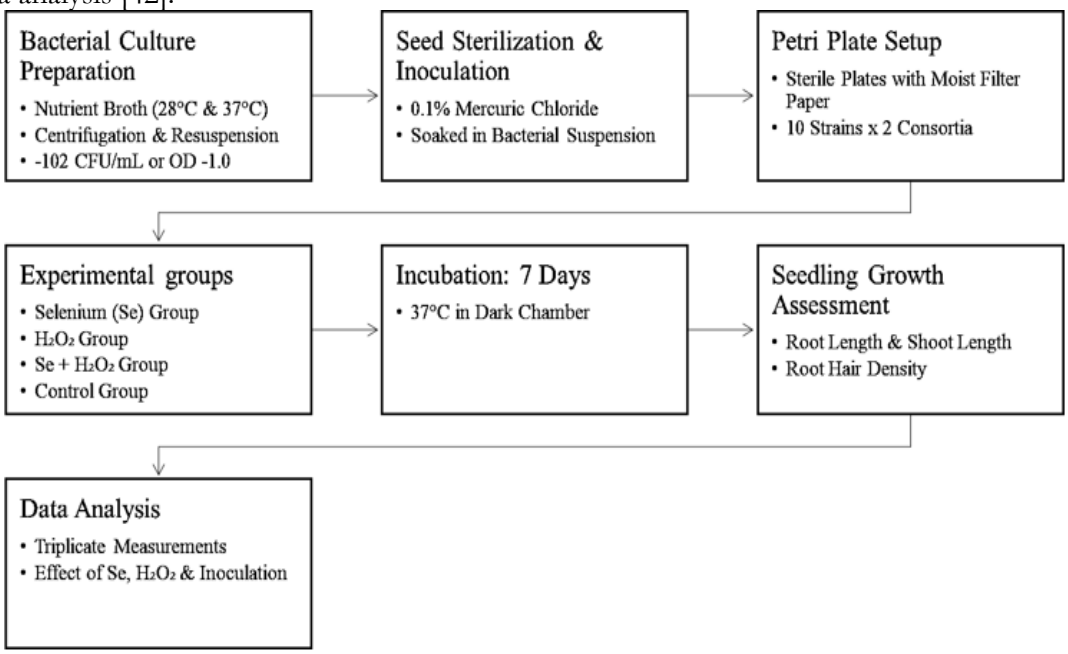

Figure 1. Effect of Bacterial Inoculum and Chemical Treatments on Seedling Growth (Se, H_2O_2 & Se + H_2O_2)

Biochemical Assays on Seedlings:

For biochemical assays, 1g of fresh seedling tissue was dissolved in cold phosphate buffer saline and centrifuged at 350 rpm for 30 min. For the malondialdehyde assay (i.e., lipid peroxidation), supernatant was combined with 0.25% Thio barbituric acid and heated at 98°C for 30 min [43]. Malondialdehyde content was measured and presented as nmol g^{-1} FW, and

optical density was measured at 450, 532, and 600 nm. This allowed for comparative quantification of oxidative damage in Z. mays seedlings among different treatments. While for the H_2O_2 assay, tissue was first homogenized in 0.1% Trichloroacetic acid and then centrifuged at 350 rpm for 30 min. Then, potassium iodide and phosphate buffer saline were added to the supernatant, and absorbance was measured at 390 nm and expressed as g^{-1} FW so that a comparison could be made between the seedling samples. [44]. Finally, for peroxidase activity, the reaction mixture, including guaiacol, H_2O_2, and enzyme extract were homogenized, and absorbance was measured at 470 nm [18]. Activity was calculated using:

$$\textbf{peroxidase activity} = \frac{\text{Absorbance of test} - \text{Absorbance of control}}{\text{Weight of sample} \times \text{Absorbance of control}}$$

The POD activity was indicated by $\Delta OD\ min^{-1}\ g^{-1}$ FW, representing the scavenging ability of ROS in seedling tissues in response to selenium and H_2O_2 stresses. These biochemical markers were used to assess oxidative stress and antioxidant responses induced by selenium, H_2O_2, and bacterial inoculation.

Results:

Isolation and Cellular Morphological Characterization of Selenium-Resistant Bacteria:

A total of 20 distinct bacterial strains were isolated from the rhizosphere soil samples by spreading dilutions on Nutrient agar, as shown in Figure 2. They were named as AFS1 to AFS6, AFS7 to AFS12, and AFS13 to AFS20, and purified using quadrant streaking. The colonies showed a variety of morphologies, edges, and surface textures. Microscopy of these isolates after Gram staining and endospore staining was performed. All twenty strains were Gram-positive rods while AFS1, AFS2, AFS4, AFS5, AFS8, AFS11, and AFS14 were spore formers and AFS3, AFS6, AFS7, AFS9, AFS10, AFS12, AFS13, AFS15, AFS16, AFS17, AFS18, AFS19, and AFS20 were non-spore-formers. This variation may be due to diverse adaptive mechanisms among strains.

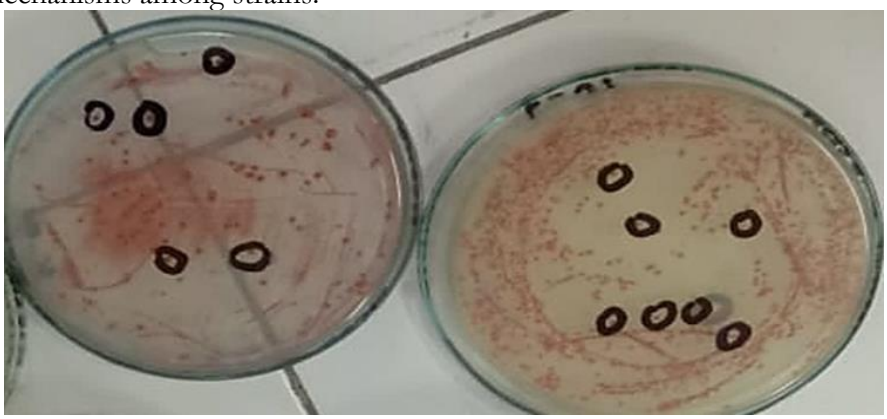

Figure 2. Selenium-resistant bacteria isolated from a soil sample

Primary Biochemical Characterization:

All of the strains AFS1 to AFS6, AFS7 to AFS12, and AFS13 to AFS20 displayed positive catalase activity, confirming the presence of peroxidase-based oxidative defense mechanisms. On the contrary, all isolates were oxidase-negative, indicating dependence on alternate electron transport pathways. Uniform positivity in Methyl Red, Voges-Proskauer, and starch hydrolysis was observed across all strains, which reveals consistent fermentative abilities and amylase activity. However, phosphate solubilization was uniformly negative in every strain, as shown in Figure 3a, showing that none of the isolates contributed significantly to phosphate degradation.

Variations were observed in advanced biochemical tests. For instance, ammonia production was positive only in strain AFS5, AFS7, AFS8, AFS11, AFS13, AFS15, AFS19, and AFS20, while strain AFS1 to AFS4, AFS6, AFS9, AFS10, AFS12, AFS14, and AFS16 to

AFS18 showed no ammonia production. Whereas, citrate solubilization was observed to be positive only in 3 strains, i.e., AFS1, AFS13, and AFS14 (Figure 3b) and negative in all other strains. Moreover, nitrate reduction was positive in strain AFS5, AFS7, AFS8, AFS11, AFS13, AFS15, AFS19, and AFS20, while negative in strain AFS1 to AFS4, AFS6, AFS9, AFS10, AFS12, AFS14, and AFS16 to AFS18. Malonate utilization was negative in all 20 isolates, demonstrating that none of the strains could use malonate as a main carbon source. Table 1 summarizes the results of staining and biochemical tests performed on all 20 strains.

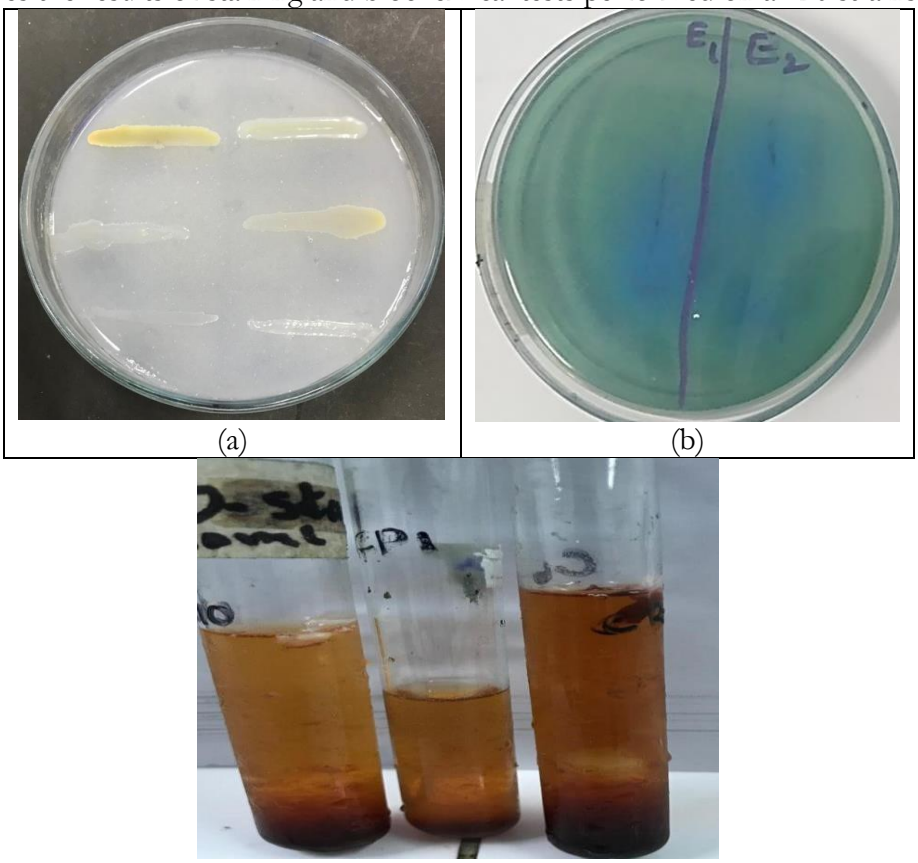

Figure 3 (a). Strains AFS2, AFS5, AFS6, AFS9, AFS12, and AFS17 were negative for phosphate solubilization. Strains AFS13 and AFS14 were positive for citrate solubilization, indicated by blue color. Strains AFS7, AFS8, and AFS11 showed positive results for nitrate reduction

Table 1. Cellular morphological characteristics using staining and biochemical characters of isolated bacterial strains using various tests.

Strain	Gram Staining	EndoSpore Staining	Catalase	Oxidase	MR-VP	Starch Hydrolysis	Phosphate Solubilization	Ammonia Production	Citrate Solubilization	Nitrate Reduction	Malonate Utilization
AFS1	+	Spore former	+	+	+	+	-	+	+	+	+
AFS2	+	Non-Spore former	-	-	+	+	-	-	-	-	-
AFS3	+	Non-Spore former	+	+	+	+	+	+	+	+	+
AFS4	+	Spore former	+	-	+	+	-	-	+	-	-
AFS5	+	Spore former	+	+	+	+	-	+	+	+	-
AFS6	+	Non-Spore former	+	-	+	+	+	+	+	+	+
AFS7	+	Non-Spore former	-	-	+	+	-	+	+	+	+
AFS8	+	Spore former	+	+	+	+	+	+	+	+	-
AFS9	+	Non-Spore former	+	-	+	+	-	+	-	+	-
AFS10	+	Spore former	+	+	+	+	+	+	+	+	+
AFS11	+	Spore former	+	-	+	+	-	+	+	+	+
AFS12	+	Spore former	+	-	+	+	-	-	-	+	-
AFS13	+	Non-Spore former	+	+	+	+	+	+	+	+	+
AFS14	+	Spore former	+	-	+	+	-	-	+	-	-
AFS15	+	Non-Spore former	+	-	+	+	+	+	+	+	+
AFS16	+	Non-Spore former	+	-	+	+	+	+	+	+	+
AFS17	+	Spore former	+	+	+	+	+	+	+	+	+
AFS18	+	Non-Spore former	+	-	+	+	-	-	-	+	-

Auxin Production and Antimicrobial Activity Against Bacillus Thuringiensis:

All strains confirmed measurable auxin production (Figure 5), and in nearly every case, auxin levels were amplified in the presence of tryptophan. AFS1, AFS2, AFS3, AFS4, AFS7, AFS8, AFS9, AFS11, AFS13, AFS15, AFS16, AFS17, AFS18, AFS19, and AFS20 all showed strong increases when tryptophan was added, while AFS5, AFS6, AFS10, AFS12, and AFS14 showed moderate changes but still produced auxin. No strain exhibited zero auxin production. Overall, all twenty strains demonstrated auxin-synthesizing ability, although the magnitude varied among strains. Antimicrobial activity against Bacillus thuringiensis differed widely, as seen in Figure 4, where several strains produced no inhibition zones and were therefore classified as negative, including AFS1, AFS2, AFS3, AFS4, AFS6, AFS8, AFS9, AFS10, AFS12, AFS14, AFS16, AFS17, and AFS18. However, AFS5, AFS7, AFS11, AFS13, AFS15, AFS19, and AFS20 displayed measurable inhibition, with AFS11 exhibiting the largest zone (17 mm). This validates that antimicrobial metabolite production is not universal but rather strain-specific.

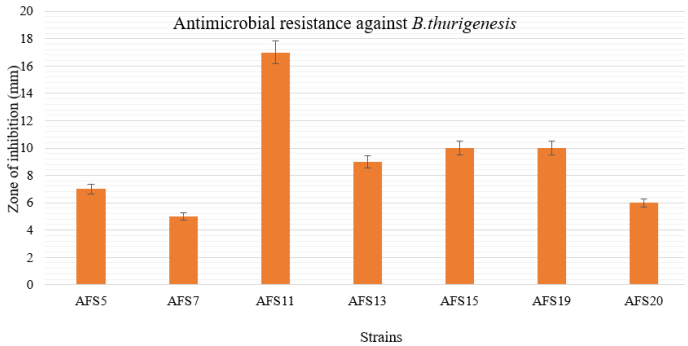

Figure 4. Antimicrobial resistance against Bacillus thurigenesis is shown by zones of inhibition in millimeters formed by 7 strains

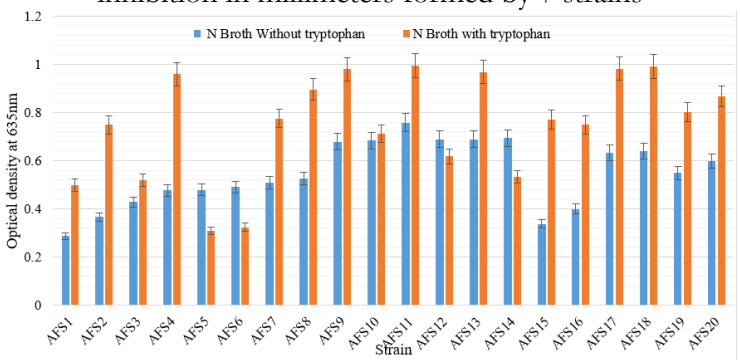

Figure 5. Auxin Production Activity**:** was evaluated in the presence and absence of tryptophan. In the presence of tryptophan, the strongest auxin production was observed in AFS11, AFS17, and AFS18, as evidenced by their highest ODs (≥ 0.99).

Selenite Reduction Potential:

All bacterial strains showed variable degrees of selenite reduction activity when subjected to increasing concentrations of sodium selenite, 100-900 µg/mL of sodium selenite. Strong reduction potential was demonstrated by strains AFS1, AFS3, AFS4, AFS7, AFS8, AFS10, AFS11, AFS12, AFS13, AFS15, AFS16, AFS17, AFS18, AFS19, and AFS20, which reached maximum optical density at provided doses. Other strains, such as AFS2, AFS5, AFS6, AFS9, and AFS14, displayed a notable decrease but showed variability dependent on concentration. No strain demonstrated zero reduction activity at any concentration, as seen in Figure 6. Controls showed negligible absorbance only, confirming that selenium reduction was a bacterial activity. Hence, the resistance and bioremediation potential of all 20 isolates were confirmed by their capability to convert selenite into selenium.

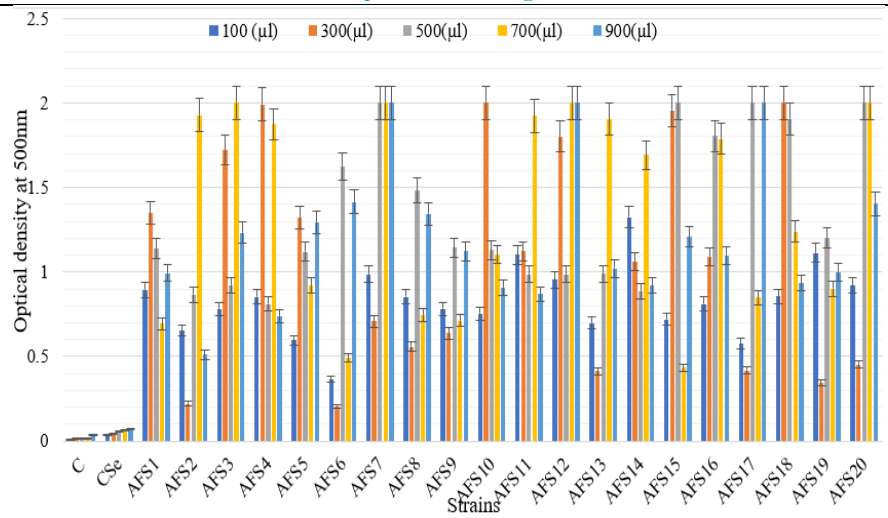

Figure 6 (a)

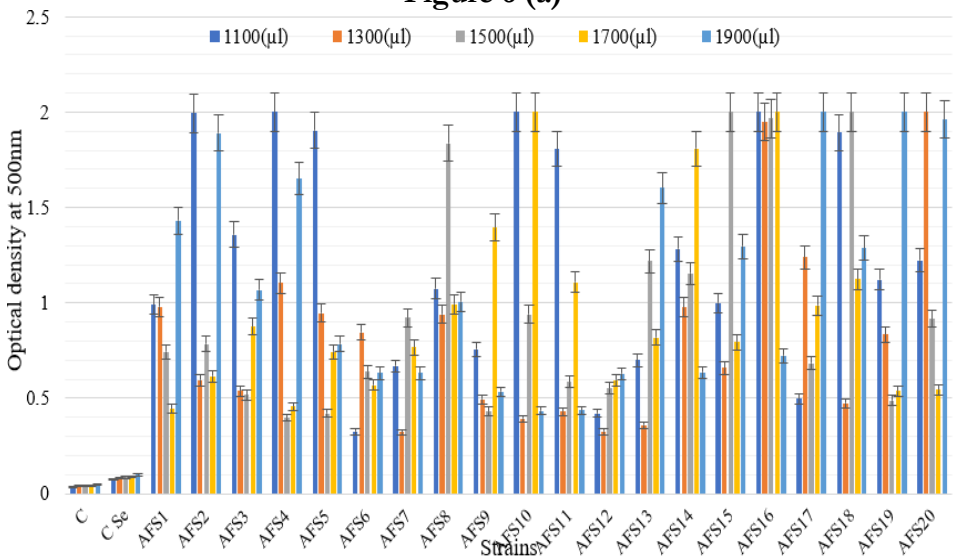

Figure 6 (b)

Figure 6: Selenium Reduction Potential (500 nm): measured at various concentrations. **a**: **Concentration 100–900 µg/mL**) shows variable reduction, with peaks at 700 µg/mL (AFS3, AFS4, AFS7, AFS12, AFS20), 500 µg/mL (AFS7, AFS18), and 900 µg/mL (AFS7, AFS12, AFS17). **b: Concentration 1100–1900 µg/mL:** shows strong reduction by AFS2, AFS4, AFS5, AFS9, AFS10, AFS11, AFS18, AFS19, and AFS20, while AFS16 remains consistently active**.**

Temperature and pH Tolerance:

All strains exhibited a variable decrease in selenium concentration under temperature stress (Figure 7). Most strains, including AFS2, AFS6, AFS8, AFS12, AFS15, AFS16, AFS17, AFS18, and AFS20, showed notably high activity at 37 °C, while almost all strains exhibited moderate activity at 28 °C, and most strains showed decreased activity at higher temperature i.e., 45 °C. However, at all three temperatures, apparent growth and selenite reduction were observed, indicating a wide range of thermal tolerance among strains. The pH experiment indicated that all isolates were able to maintain optimal activity at acidic pH 5, neutral pH 7, and alkaline pH 9, whereas strain AFS1, AFS2, AFS3, AFS6, AFS9, AFS11, AFS15, AFS16, AFS17, AFS18, and AFS19 attained optical densities of up to 2.0 at all three pH ranges. Other strains showed moderate but consistent activity. No strain was inactive at any pH**,** indicating broad environmental adaptability (Figure 8).

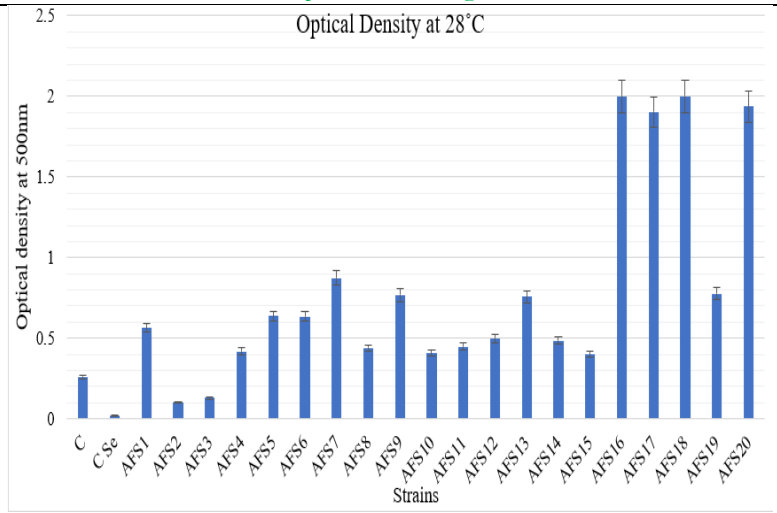

Figure 7 (a)

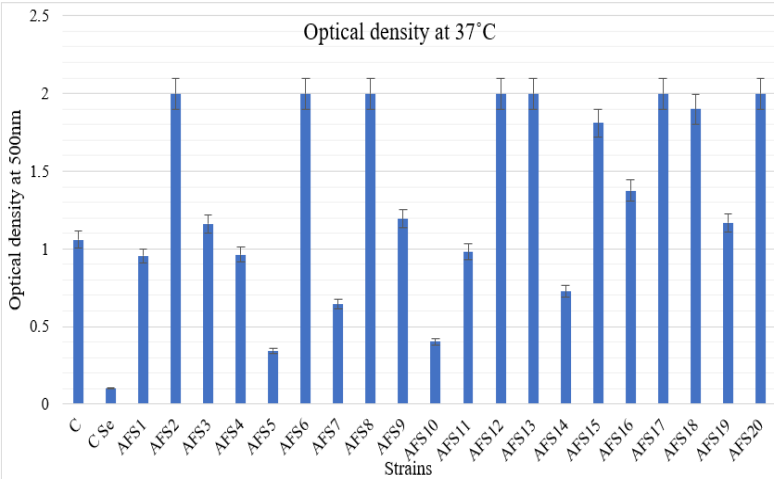

Figure 7 (b)

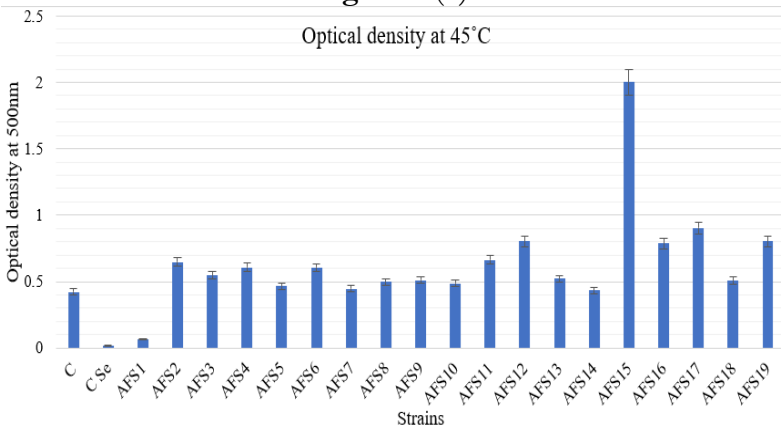

Figure 7©

Figure 7. Temperature Tolerance at 500nm: it displays growth (OD) at 28˚C, 37˚C & 45˚C compared with the control without selenium (C) and control with selenium (CSe). **Figure 7a: OD at 28°C** where AFS16, AFS17, AFS18, and AFS20 show maximum growth **Figure 7b: OD at 37°C** where strain AFS2, AFS6, AFS8, AFS12, AFS17, and AFS20 show high peaks **Figure 7c: OD at 45°C** shows trend that overall growth is suppressed for most strains but AFS15 shows very high growth, suggesting it may be thermophilic or highly heat-tolerant.

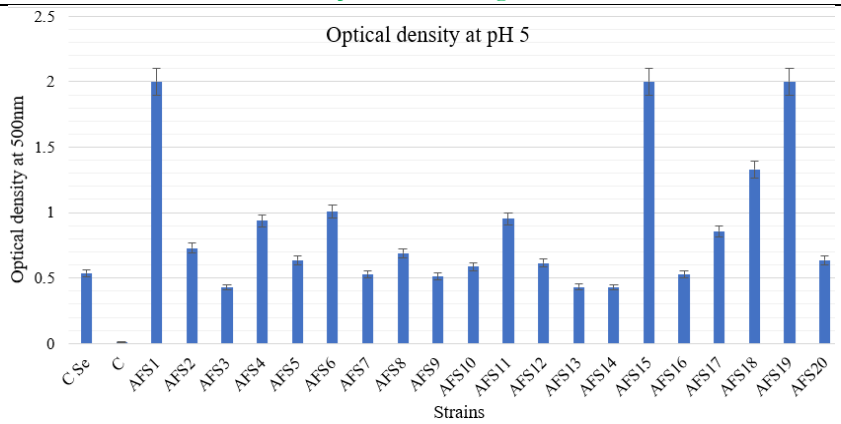

Figure 8 (a)

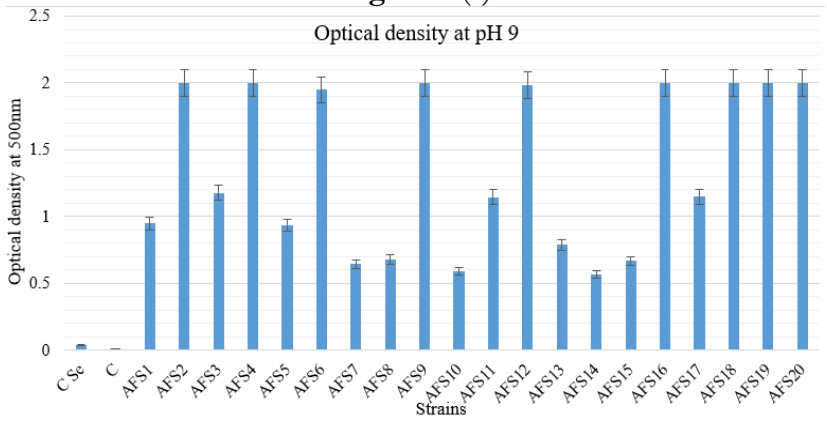

Figure 8 (b)

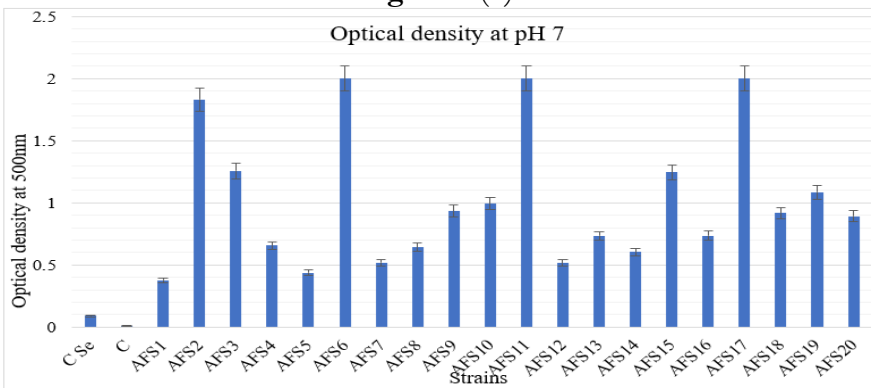

Figure 8 (c)

Figure 8: **pH Tolerance at 500nm:** It displays growth (OD) at pH 5, pH 7, and pH compared with the control without selenium (C) and the control with selenium (CSe). **a: OD at pH 5 (Acidic):** Growth is variable, while strains AFS1, AFS15, AFS18, and AFS19 show the highest tolerance. **b: OD at pH 9 (Alkaline):** strain AFS2, AFS4, AFS6, AFS9, AFS12, AFS16, AFS18-20 all reach high optical densities. **c: OD at pH 7 (Neutral)**: Notable peaks (highest growth) are seen in strain AFS2, AFS6, AFS11, and AFS17**.**

Heavy Metal Resistance:

When subjected to heavy metal stress by using Co, Zn, Hg, Ni, Mn, Cu, Pb, Mg, Li, Fe, and $K_2Cr_2O_7$, almost all strains demonstrated varying resistance as seen in Table 2. Strains such as AFS2, AFS3, AFS4, AFS5, AFS7, AFS9, AFS10, AFS15, AFS16, AFS17, AFS18, AFS19, and AFS20 exhibited abundant growth for many metals. Other strains like AFS1, AFS6, AFS8, AFS11, AFS12, AFS13, and AFS14 showed multi-metal resistance but with moderate growth. None of the strains showed complete metal sensitivity, confirming strong environmental adaptation.

Table 2. Heavy Metal Resistance Profile of Selenite Reducing Bacterial strains at 1% Heavy metals (400µg/ml) of each metal including Cobalt (Co) Copper (Cu), Iron (Fe), Lead (Pb), Lithium (Li), Magnesium (Mg), Manganese (Mn), Mercury (Hg), Nickel (Ni), Potassium dichromate ($K_2Cr_2O_7$) and Zinc (Zn) shown as ++++ (abundant growth), +++ (adequate growth), ++ (less abundant growth), + (least growth), ND (not detected)

Strain	Co	Cu	Fe	Pb	Li	Mg	Mn	Hg	Ni	K2Cr2O7	Zn
AFS1	+	+++	++++	++++	++++	++++	++++	+++	+++	+++	++++
AFS2	++++	++++	++++	++++	++++	++++	++++	++++	++++	++++	++++
AFS3	ND	+++	++++	++++	++++	++++	++++	++++	++++	++++	++++
AFS4	++++	+	++++	++++	++++	++++	++++	+	++++	++	++++
AFS5	+++	++++	++++	++++	++++	++++	+	++++	++++	+	++++
AFS6	++++	++++	++++	++++	++++	++++	++++	++++	++++	+	++++
AFS7	++++	++++	++++	++++	++++	++++	++++	++++	+	+	++++
AFS8	ND	++++	++++	++++	++++	++++	++++	+++	++++	++++	++++
AFS9	++++	++++	++++	++++	++++	++++	++++	+++	ND	++++	++++
AFS10	++++	++++	++++	++++	++++	++++	+++	+	++	++++	++++
AFS11	++++	++++	++++	++++	++++	++++	++++	++	++	++++	++++
AFS12	ND	++++	++++	++++	++++	++++	+++	++	++	++++	++++
AFS13	ND	++++	++++	++++	++++	++++	++++	+++	++	++++	++++
AFS14	ND	++++	++++	++++	++++	++++	+	ND	++++	++++	++++
AFS15	++++	++++	++++	++++	++++	++++	++++	+++	++	++++	++
AFS16	++++	++++	++++	++++	++++	++++	++++	++++	++	++++	++++
AFS17	+++	++++	++++	++++	++++	++++	+	+++	++	++++	++++
AFS18	ND	++++	++++	++++	++++	++++	++++	+++	++	++++	++++
AFS19	++++	++++	++++	++++	++++	++++	++++	+++	++	++++	++++
AFS20	ND	++++	++++	+++	++	++++	++++	++	++	++	++++

Effect of Selenium and H2O2 on Zea mays L. Seedlings:

Almost all strains enhanced seedling growth under selenium, hydrogen peroxide, and combined stress conditions when compared with untreated control as shown in Figure 9. Strains AFS1, AFS3, AFS6, AFS13, AFS15, AFS16, AFS17, AFS18, AFS19, and AFS20 produced longer shoots and roots. It was noted that even strains with lower performance contributed to measurable growth enhancement. Root hair formation also exhibited universal improvement across all strains.

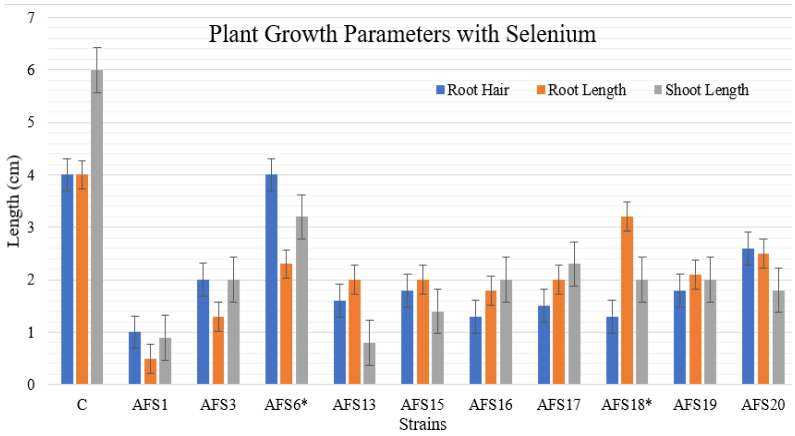

Figure 9 (a)

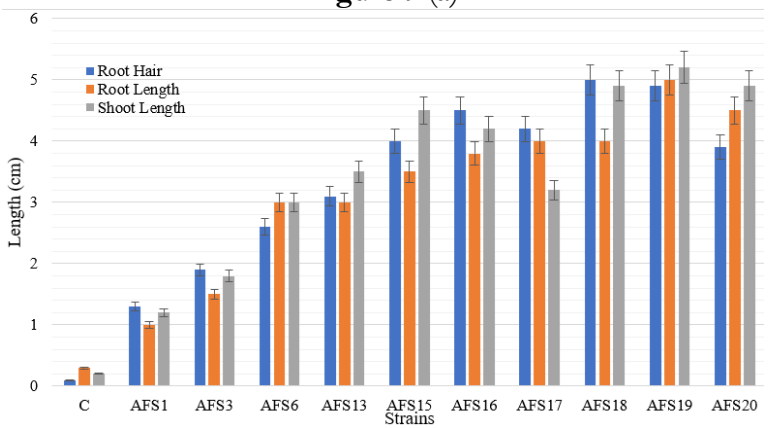

Figure 9 (b)

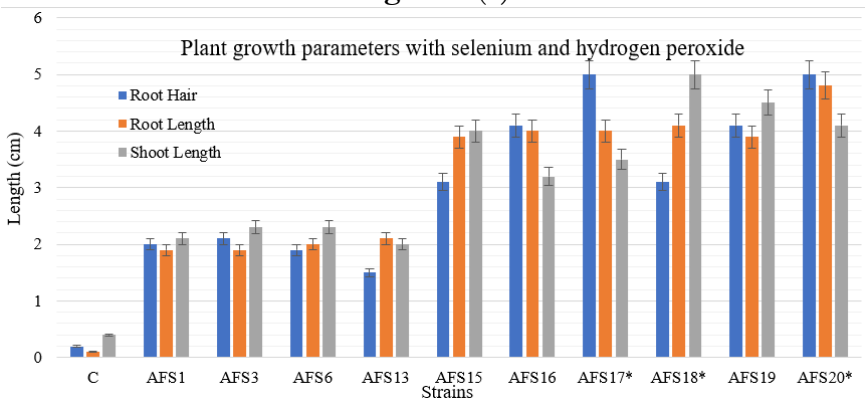

Figure 9 (c)

Figure 9. Plant Growth Parameters (cm): These Figures measure root hair length, root and shoot length of Zea mays treated with different strains under different chemical stress. **Figure 9 a: Selenium Stress**: strain AFS6 shows the best root hair length, while strain AFS18 shows the best Root Length. **b: Hydrogen Peroxide Stress**: shows linear improvement in growth metrics from strain AFS1 through AFS20. **c: Selenium** and

Hydrogen Peroxide Stress strains (specifically AFS17, AFS20) perform best, maintaining high root and shoot lengths despite the combined chemical stresses.

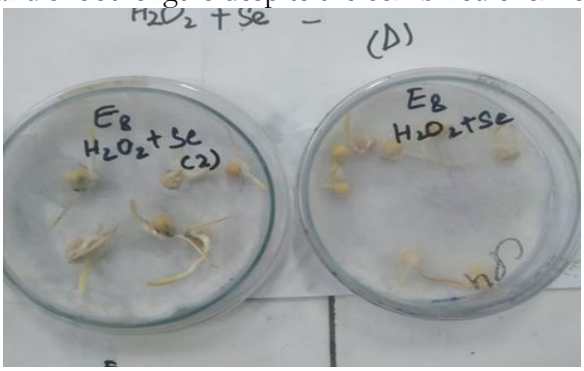

Figure 10. Seed germination of Zea mays on petri dishes with a double layer of filter papers augmented with H_2O_2 and Selenium after 6 days

Oxidative Stress Biochemistry in Seedlings (Peroxidase, H_2O_2 and Malondialdehyde):

Every strain influenced oxidative stress indicators, as shown in Figures 11 and 12. H_2O_2 content also reduced 20–45% under inoculation treatments for all strains, but each strain differed in effectiveness. Malondialdehyde levels rose under stress but dropped about 25–50% upon inoculation with any of the twenty strains. Strains AFS15, AFS16, AFS17, AFS18, AFS19, and AFS20 exhibiting higher activity, while AFS1, AFS3, AFS6, AFS13, and AFS15 indicated moderate effects. All of the bacterial isolates caused a considerable increase in peroxidase levels in seedlings treated with them. Strains AFS16, AFS17, AFS18, AFS19, and AFS20 showed the highest increases. However, the concomitant increase in peroxidase activity indicates the protective role of selenium-resistant rhizobacteria on the cellular redox states of the oxidative stress-treated seedlings.

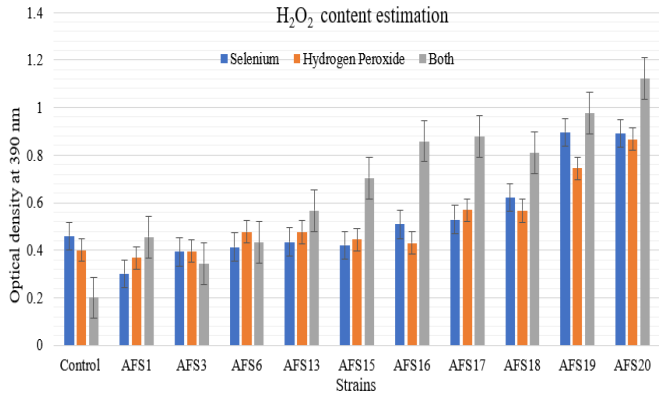

Figure 11 (a)

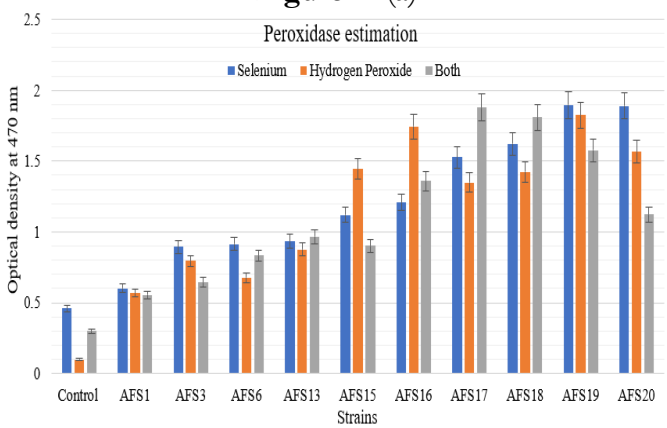

Figure 11 (b)

Figure 11. H_2O_2 content measurement and POD Estimation. a: H_2O_2 estimation at 390nm: There is a steady increase with Strain AFS20 showing the highest values across all conditions, particularly in the combined stress condition. **b: POD Estimation at 470nm:** Strain AFS19 and AFS20 show the highest activity under Selenium stress, while AFS15 shows a distinct spike under Hydrogen Peroxide stress.

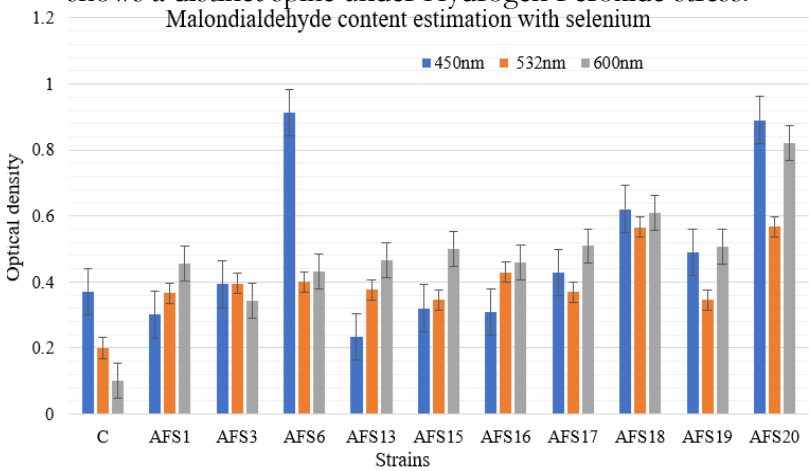

Figures 12 (a)

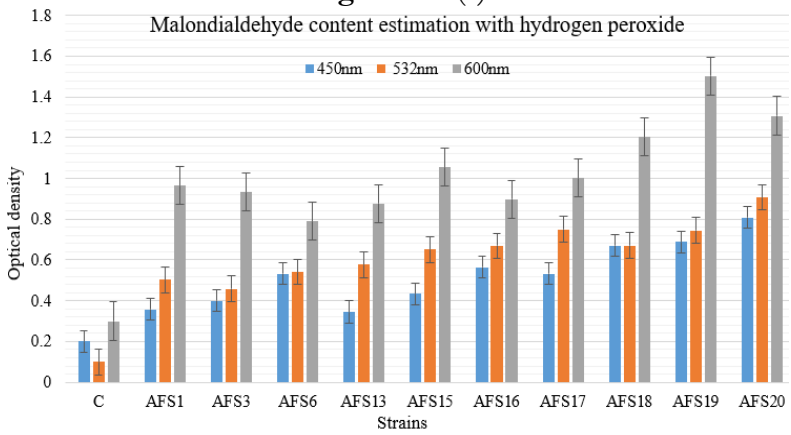

Figures 12 (b)

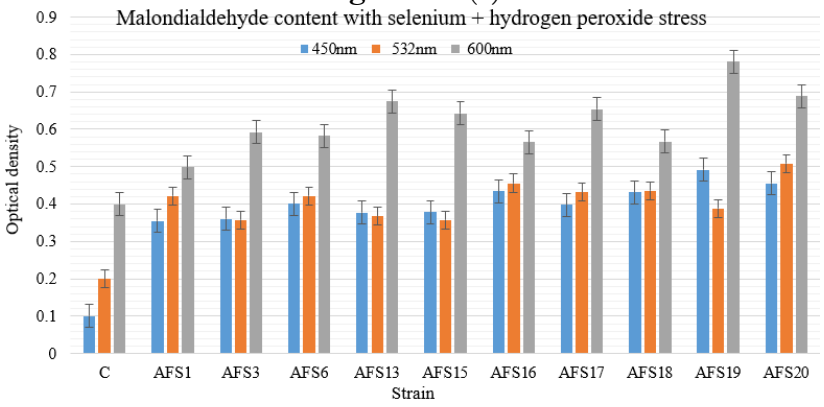

Figures 12 (c)

Figures 12. Malondialdehyde Content (MDA) under different chemical stress at three different O.D at 450nm, 532nm & 600nm**: Selenium Stress** strain AFS6 shows a significant spike at 450nm, while AFS20 shows higher density at 450nm and 600nm. **b: Hydrogen Peroxide Stress:** AFS19 and AFS20 are showing the highest optical density, at 600nm, suggesting strong stress tolerance. **c: Selenium and Hydrogen Peroxide Stress:** shows

that under combined stress, the overall optical density is lower than in single stress conditions

Discussions:

The isolation of twenty Gram-positive, catalase-positive, and oxidase-negative bacterial strains from selenium-rich rhizosphere soils. It demonstrates the presence of a specialized microbial community equipped to withstand significant selenium stress. The phenotypic variety, i.e., eight spore-forming isolates, directs resistance to extreme environmental conditions. Which is similar to observations from selenium-tolerant Priestia spp. isolated from polluted soils (47). The presence of uniform MR^+/VP^+ activity and starch hydrolysis indicates metabolic adaptability. Selective strains also demonstrated the ability to reduce nitrate and produce ammonia, suggesting a role in nutrient cycling.

The significant auxin production found in several strains supports recent findings that auxin-producing and selenium-resistant bacteria improve root structure and stress tolerance during heavy metal exposure [45]. Strain AFS11 showed most antimicrobial activity against Bacillus thuringiensis, which collaborates with previous research, i.e., selenium tolerating growth enhancing rhizobacteria frequently exhibit broad-spectrum antimicrobial activities [46].

Strains showed selenium tolerance up to 1900 μg/mL compared to formerly documented selenium-resistant PGPR, such as Priestia sp. LWS1 [47]. This shows the presence of effective detoxification mechanisms such as efflux systems, selenite reduction, or biotransformation. Similar methods have also been observed in Sinorhizobium meliloti 1021, which converts selenite to selenium nanoparticles using the reductive pathways [48]. Strong multi-metal resistance confirms adaptation capabilities to different heavy metal-contaminated environments. By preserving microbial activity and promoting plant growth in areas under heavy metal contamination, these bacteria can improve soil resilience. Their potential uses in phytoremediation and bioremediation techniques for contaminated agroecosystems are suggested by their combined metal tolerance and selenite-reducing capacity. This supports recent findings emphasizing the function of multi-metal-resistant PGPR in phytoremediation [49].

The observed enhancement in Zea mays seedling growth closely aligned with the auxin production capacity of the selenium-resistant bacterial strains. High auxin-producing strains AFS17-AFS20 promoted prominent root elongation and root hair density, which are known auxin-regulated traits. These traits likely improved water and nutrient absorption, thereby reinforcing antioxidant defense and growth resilience. These findings match recent research, i.e., selenium-associated rhizobacteria improve plant tolerance by transforming antioxidant defenses and lowering oxidative membrane damage [50]. After bacterial supplementation, malondialdehyde levels were reduced, and antioxidant activity increased, indicating improved redox equilibrium. Greater peroxidase activity confirms previous research related to PGPR-mediated enzyme activation for abiotic stress management [51].

Strains AFS19-AFS20 and AFS15 were prominent due to their combined selenium tolerance, multi-metal resistance, auxin production, antioxidant induction, and evident progress in plant development. Their characteristics match previous studies regarding microbial selenium bioremediation [52], nanoparticle-assisted stress reduction [53], and multi-metal phytoremediation techniques. Future research in this field should work on the discovery of genes responsible for selenium reduction and oxidative stress tolerance. Omics-driven analyses have recently revealed reductase systems and regulatory genes in selenium-transforming rhizobacteria [54][55]. Rigorous field testing and dedicated work on formulation development will be necessary for practical application for agriculture or bioremediation.

Conclusion:

Selenium and H_2O_2 cause oxidative stress in Zea mays L. seedlings but also trigger antioxidant defense pathways. Selenium and H_2O_2 work as an antioxidant at controlled concentrations. Their mutual influence can be synergistic or antagonistic depending upon concentration and exposure conditions, signifying the complexities of plant redox biology. Selenium-rich rhizosphere soils support selenium-resistant bacterial strains with an extensive range of biochemical capabilities, metabolic features, and resistance levels, and convert toxic selenium species into less damaging or even beneficial ones. These bacteria have the potential for bioremediation and phytostimulation, and how they interact may affect selenium uptake and stress responses in Zea mays. Future research ought to focus on molecular identification and functional gene characterization of the most efficient selenium-resistant strains and biosafety assessments through controlled field trials. Additionally, the development of stable microbial bioformulations will be essential to translate these findings into practical agricultural and bioremediation applications.

References:

[1] J. H. Shouran Wang, "Effects of hydrogen peroxide priming on yield, photosynthetic capacity and chlorophyll fluorescence of waterlogged summer maize," *Front. Plant Sci.*, vol. 13, 2022, [Online]. Available: https://www.frontiersin.org/journals/plant-science/articles/10.3389/fpls.2022.1042920/full

[2] N. S.-M. Temesgen Assefa Gelaw, "Molecular priming with H2O2 and proline triggers antioxidant enzyme signals in maize seedlings during drought stress," *Biochim. Biophys. Acta - Gen. Subj.*, vol. 1868, p. 130633, 2024, [Online]. Available: https://www.sciencedirect.com/science/article/abs/pii/S030441652400076X#:~:text=Seed-priming with H2,radicals (O2−).

[3] B. Z. Juan Hu, Baizhao Ren, Shuting Dong, Peng Liu, "Comparative proteomic analysis reveals that exogenous 6-benzyladenine (6-BA) improves the defense system activity of waterlogged summer maize," *BMC Plant Biol.*, vol. 20, no. 44, 2020, [Online]. Available: https://link.springer.com/article/10.1186/s12870-020-2261-5

[4] Alberto Marco Del Pino, Beatrice Falcinelli, "In Vitro Oxidative Stress Threatening Maize Pollen Germination and Cytosolic Ca2+ Can Be Mitigated by Extracts of Emmer Wheatgrass Biofortified with Selenium," *Plants (Basel, Switzerland)*, vol. 11, no. 7, 2022, [Online]. Available: https://pubmed.ncbi.nlm.nih.gov/35406839/

[5] D. C. Zesmin Khan, Thorny Chanu Thounaojam, "The role of selenium and nano selenium on physiological responses in plant: a review," *Plant Growth Regul.*, vol. 100, pp. 409–433, 2023, [Online]. Available: https://link.springer.com/article/10.1007/s10725-023-00988-0

[6] M. Yildiz, E. Pehlivan, and H. Terzi, "Selenium Toxicity Induced Physiological and Biochemical Alterations in Maize Seedlings," *Eur. J. Biol.*, vol. 82, no. 2, pp. 154–160, 2023, doi: 10.26650/EURJBIOL.2023.1353293.

[7] Muhammad Ishtiaq, Muhammad Waqas Mazhar, "Seed Priming with the Selenium Nanoparticles Maintains the Redox Status in the Water Stressed Tomato Plants by Modulating the Antioxidant Defense Enzymes," *Plants*, 2023, [Online]. Available: https://pmc.ncbi.nlm.nih.gov/articles/PMC10096850/

[8] Qinyong Dong, Tingjie Huang, "Nano-priming with selenium nanoparticles reprograms seed germination, antioxidant defense, and phenylpropanoid metabolism to enhance Fusarium graminearum resistance in maize seedlings," *J. Adv. Res.*, 2025, [Online]. Available: https://www.sciencedirect.com/science/article/pii/S2090123225003789

[9] Wang Zhike, "Exogenous H2O2 alleviates maize seed germination and seedling physiology property under drought stress," *ResearchGate*, 2025, [Online]. Available: https://www.researchgate.net/publication/389931136_Exogenous_H2O2_alleviates_maize_seed_germination_and_seedling_physiology_property_under_drought_stress

[10] S. O. Hasna Ellouzi, "Seed-priming with H2O2 alleviates subsequent salt stress by preventing ROS production and amplifying antioxidant defense in cauliflower seeds and seedlings," *Sci. Hortic. (Amsterdam).*, vol. 288, p. 110360, 2021, [Online]. Available:

https://www.sciencedirect.com/science/article/abs/pii/S0304423821004672

[11] Chukwuebuka Egbuna, Kingsley C. Patrick-Iwuanyanwu, "Analytical Techniques in Biosciences: From Basics to Applications," *Acad. Press*, 2022, [Online]. Available: https://www.sciencedirect.com/book/edited-volume/9780128226544/analytical-techniques-in-biosciences

[12] H. J. Benson, "Microbiological applications : laboratory manual in general microbiology : Benson, Harold J : Free Download, Borrow, and Streaming : Internet Archive," Boston : McGraw-Hill. Accessed: Jan. 21, 2026. [Online]. Available: https://archive.org/details/microbiologicala0000bens_h8x6

[13] J. G. Cappuccino, "Microbiology : a laboratory manual : Cappuccino, James G : Free Download, Borrow, and Streaming : Internet Archive," San Francisco : Pearson/Benjamin Cummings. Accessed: Jan. 21, 2026. [Online]. Available: https://archive.org/details/microbiologylabo0000capp_v2t7

[14] Sagar Aryal, "Streak Plate Method: Principle, Types & Step-by-Step Guide," Microbe Notes. Accessed: Jan. 21, 2026. [Online]. Available: https://microbenotes.com/streak-plate-method-principle-methods-significance-limitations/

[15] N. Tripathi, M. Zubair, and A. Sapra, "Gram Staining," *StatPearls [Internet]*, Mar. 2025, Accessed: Jan. 21, 2026. [Online]. Available: https://www.ncbi.nlm.nih.gov/books/NBK562156/

[16] T. Mittwer, J. W. Bartholomew, and B. J. Kallman, "The Mechanism of the Gram Reaction. II. The Function of Iodine in the Gram Stain," *Stain Technol.*, vol. 25, no. 4, pp. 169–179, 1950, doi: 10.3109/10520295009110986.

[17] A. B. Schaeffer and M. D. Fulton, "A Simplified Method Of Staining Endospores," *Science*, vol. 77, no. 1990, p. 194, 1933, doi: 10.1126/SCIENCE.77.1990.194.

[18] A. C. MAEHLY and B. CHANCE, "The assay of catalases and peroxidases.," *Methods Biochem. Anal.*, vol. 1, pp. 357–424, 1954, doi: 10.1002/9780470110171.CH14;PAGEGROUP:STRING:PUBLICATION.

[19] Sagar Aryal, "Oxidase Test- Principle, Uses, Procedure, Types, Result Interpretation...," Microbiology. Accessed: Jan. 21, 2026. [Online]. Available: https://microbiologyinfo.com/oxidase-test-principle-uses-procedure-types-result-interpretation-examples-and-limitations/

[20] K. R. Morakot Krajang, Kwanruthai Malairuang, Jatuporn Sukna, "Single-step ethanol production from raw cassava starch using a combination of raw starch hydrolysis and fermentation, scale-up from 5-L laboratory and 200-L pilot plant to 3000-L industrial fermenters," *Biotechnol. Biofuels*, vol. 14, no. 68, 2021, [Online]. Available: https://link.springer.com/article/10.1186/s13068-021-01903-3

[21] A. M. A. Shaikhul Islam, "Isolation and Identification of Plant Growth Promoting Rhizobacteria from Cucumber Rhizosphere and Their Effect on Plant Growth Promotion and Disease Suppression," *Front. Microbiol.*, 2026, [Online]. Available: https://www.frontiersin.org/journals/microbiology/articles/10.3389/fmicb.2015.01360/full

[22] C. Y. and B. M. YS Ismail, "Characterization of lactic acid bacteria from local cow´s milk kefir," *IOP Conf. Ser. Earth Environ. Sci.*, vol. 130, no. 1, 2019, [Online]. Available: https://iopscience.iop.org/article/10.1088/1755-1315/130/1/012019

[23] Sagar Aryal, "Voges-Proskauer (VP) Test: Principle, Procedure & Results," Biochemical Test. Accessed: Jan. 21, 2026. [Online]. Available: https://microbenotes.com/voges-proskauer-vp-test/

[24] M. E. M.-H. Ma Esther Sanchez-Gonzalez, "Effect of pH and Carbon Source on Phosphate Solubilization by Bacterial Strains in Pikovskaya Medium," *Microorganisms*, vol. 11, no. 1, p. 49, 2023, [Online]. Available: https://www.mdpi.com/2076-2607/11/1/49

[25] Rebecca Buxton, "Nitrate and Nitrite Reduction Test Protocols," *Am. Soc. Microbiol.*, 2011, [Online]. Available: https://asm.org/asm/media/protocol-images/nitrate-and-nitrite-reduction-test-protocols.pdf?ext=.pdf

[26] S. Abdelwahed *et al.*, "A new pioneer colorimetric micro-plate method for the estimation of ammonia production by plant growth promoting rhizobacteria (PGPR)," *Main Gr. Chem.*, vol.

21, no. 1, pp. 55–68, 2022, doi: 10.3233/MGC-210077.

[27] M. D. R. G. da S. Sara Porfírio, "Current analytical methods for plant auxin quantification – A review," *Anal. Chim. Acta*, vol. 902, pp. 8–21, 2016, [Online]. Available: https://www.sciencedirect.com/science/article/abs/pii/S0003267015013148

[28] K. B. Moamen M. Elmassry, "Malonate utilization by Pseudomonas aeruginosa affects quorum-sensing and virulence and leads to formation of mineralized biofilm-like structures," *Mol. Microbiol.*, 2021, [Online]. Available: https://pubmed.ncbi.nlm.nih.gov/33892520/

[29] E. M. Jenny Åhman, "Evaluation of ten brands of pre-poured Mueller-Hinton agar plates for EUCAST disc diffusion testing," *Clin. Microbiol. Infect.*, vol. 28, no. 11, 2022, [Online]. Available: https://www.sciencedirect.com/science/article/pii/S1198743X22002890

[30] M. Balouiri, M. Sadiki, and Saad Koraichi Ibnsouda, "Methods for in vitro evaluating antimicrobial activity: A review," *J. Pharm. Anal.*, vol. 6, no. 2, 2016, [Online]. Available: https://www.sciencedirect.com/science/article/pii/S2095177915300150

[31] N. B. Rabia Shahdin, "Isolating Indigenous Metal Resistant Gram-Positive Bacteria: Assessing Their Selenite Reduction Potential," *J. Microbiol. Mol. Genet.*, 2024, [Online]. Available: https://jmmg.wum.edu.pk/index.php/ojs/article/view/159

[32] E. M. Vira Hovorukha, "Metal Resistance of Microorganisms as a Crucial Factor for Their Homeostasis and Sustainable Environment," *Sustainability*, vol. 16, no. 22, p. 9655, 2024, [Online]. Available: https://www.mdpi.com/2071-1050/16/22/9655

[33] ImplicationsPDF and L. U. G.-A. Carlos G. Sánchez-Corona, "Impact of Heavy Metal and Resistance Genes on Antimicrobial Resistance: Ecological and Public Health Implications," *Genes (Basel)*, vol. 16, no. 6, p. 625, 2025, [Online]. Available: https://pubmed.ncbi.nlm.nih.gov/40565518/

[34] B. K. S. Vivek Roy, "Isolation, characterization, identification, genomics and analyses of bioaccumulation and biosorption potential of two arsenic-resistant bacteria obtained from natural environments," *Sci. Rep.*, vol. 14, no. 1, 2024, [Online]. Available: https://pubmed.ncbi.nlm.nih.gov/38459150/

[35] Marynes Quintero, Sol D. Zuluaga-Valencia, "Mercury-Resistant Bacteria Isolated from an Estuarine Ecosystem with Detoxification Potential," *Microorganisms*, vol. 12, no. 12, p. 2631, 2024, [Online]. Available: https://www.mdpi.com/2076-2607/12/12/2631

[36] A. A. de Lima e Silva *et al.*, "Heavy metal tolerance (Cr, Ag AND Hg) in bacteria isolated from sewage," *Braz. J. Microbiol.*, vol. 43, no. 4, pp. 1620–1631, Oct. 2012, doi: 10.1590/S1517-838220120004000047.

[37] J. B. Glass, "Metals, microbes, and minerals: the biogeochemical side of life, vol. 21 of metal ions in life ," *Transit. Met. Chem. 2021 466*, vol. 46, no. 6, pp. 423–426, May 2021, doi: 10.1007/S11243-021-00462-8.

[38] C. U. A. Nnabueze Darlington Nnaji, "Mechanisms of Heavy Metal Tolerance in Bacteria: A Review," *Sustainability*, vol. 16, no. 24, p. 11124, 2024, [Online]. Available: https://www.mdpi.com/2071-1050/16/24/11124

[39] H. C. Hannah Johnson, "Bacterial Heavy Metal Resistance Genes and Bioremediation Potential," *Comput. Mol. Biosci.*, vol. 9, no. 1, pp. 1–12, 2019, [Online]. Available: https://www.researchgate.net/publication/331252311_Bacterial_Heavy_Metal_Resistance_Genes_and_Bioremediation_Potential

[40] E. A. Gilvanova and P. Y. Milman, "Biosynthesis of auxin and carotene during the growth of PGPR-bacteria Pantoea sp. on nutrient media of different composition," *Biomics*, vol. 12, no. 2, pp. 218–2223, 2020, doi: 10.31301/2221-6197.BMCS.2020-12.

[41] A. Varma and A. Jain, "Protocol for Seed Surface Sterilization and In Vitro Cultivation," *Biol. Biotechnol. Quinoa Super Grain Food Secur.*, pp. 265–282, Jan. 2021, doi: 10.1007/978-981-16-3832-9_13.

[42] Y. Q. Haiyun Li, "Effects of PGPR microbial inoculants on the growth and soil properties of Avena sativa, Medicago sativa, and Cucumis sativus seedlings," *Soil Tillage Res.*, vol. 199, p. 104577, 2020, [Online]. Available: https://www.sciencedirect.com/science/article/abs/pii/S0167198719306968

[43] Robert L. Heath, Lester packer, "Reprint of: Photoperoxidation in Isolated Chloroplasts I.

Kinetics and Stoichiometry of Fatty Acid Peroxidation," *Arch. Biochem. Biophys.*, vol. 726, p. 109248, 2022, [Online]. Available: https://www.sciencedirect.com/science/article/abs/pii/S0003986122001333

[44] S. ES and M. S, "Protective Effect of Some Local Plants against Oxidative Stress Caused by Hydrogen Peroxide," *J. Environ. Toxicol. Stud.*, vol. 1, no. 1, 2017, doi: 10.16966/2576-6430.104.

[45] Q. Chen, X., Wang, J., Li, "Auxin-producing rhizobacteria enhance plant tolerance to selenium toxicity by regulating antioxidant metabolism," *Environ. Res.*, vol. 216, p. 114645, 2023.

[46] M. Alkhalifa, A., Alharbi, O., Alqarni, "Antimicrobial potential of selenium-tolerant plant-growth-promoting bacteria isolated from contaminated soils," *Appl. Sci.*, vol. 11, no. 14, p. 6529, 2021.

[47] Z. Liu, Y., Sun, J., Hu, "Physiological and genomic insights into selenium-tolerant Priestia sp. and its role in selenium biofortification," *Front. Microbiol.*, vol. 13, p. 950211, 2022.

[48] H. Gao, Y. Ji, and W. Chen, "Selenite resistance and biotransformation to SeNPs in Sinorhizobium meliloti 1021 and the synthetic promotion on alfalfa growth," *Microbiol. Res.*, vol. 280, p. 127568, 2024, [Online]. Available: https://www.sciencedirect.com/science/article/pii/S0944501323002707

[49] A. Gupta, R., Singh, "Multi-metal-tolerant PGPR in phytoremediation: Mechanisms, applications, and recent advances," *Microorganisms*, vol. 12, no. 4, p. 700, 2021.

[50] C. H. Yin Wang, "Selenium-induced rhizosphere microorganisms endow salt-sensitive soybeans with salt tolerance," *Environ. Res.*, vol. 236, p. 116827, 2023, [Online]. Available: https://www.sciencedirect.com/science/article/abs/pii/S0013935123016316

[51] Y. C. Yong Qi Liu, "Plant growth-promoting bacteria modulate gene expression and induce antioxidant tolerance to alleviate synergistic toxicity from combined microplastic and Cd pollution in sorghum," *Ecotoxicol. Environ. Saf.*, vol. 264, p. 115439, 2023, [Online]. Available: https://www.sciencedirect.com/science/article/pii/S0147651323009430

[52] H. B. C. Xiao Rui Lin, "Priestia sp. LWS1 Is a Selenium-Resistant Plant Growth-Promoting Bacterium That Can Enhance Plant Growth and Selenium Accumulation in Oryza sativa L," *Agronomy*, vol. 12, no. 6, p. 1301, 2022, [Online]. Available: https://www.mdpi.com/2073-4395/12/6/1301

[53] P. A. Akhtar, Nosheen, Noshin Ilyas, Zia-ur-Rahman Mashwani, Rifat Hay, Humaira Yasmin, Ahmed Noureldeen, "Synergistic effects of plant growth promoting rhizobacteria and silicon dioxide nano-particles for amelioration of drought stress in wheat," *Plant Physiol. Biochem.*, vol. 166, pp. 160–176, 2021, doi: https://doi.org/10.1016/j.plaphy.2021.05.039.

[54] M. Z. Ruixin Fu, "Harnessing the Rhizosphere Microbiome for Selenium Biofortification in Plants: Mechanisms, Applications and Future Perspectives," *Microorganisms*, vol. 13, no. 6, p. 1234, 2025, [Online]. Available: https://www.mdpi.com/2076-2607/13/6/1234

[55] S. N. Michela Schiavon, "Selenium biofortification in the 21st century: status and challenges for healthy human nutrition," *Plant Soil*, vol. 453, no. 1–2, pp. 245–270, 2020, [Online]. Available: https://pubmed.ncbi.nlm.nih.gov/32836404/